Networked Cooperative Marine Vehicle Control using Acoustic and Optical Communications

Ana Catarina Silvestre
anacsilvestre@tecnico.ulisboa.pt

Instituto Superior Técnico, Lisboa, Portugal

November 2020

Abstract

The first part of this work addresses the problem of cooperative control of multiple vehicles, with a special focus on cooperative path following and motion control of a network of vehicles interconnected using acoustic or optical communication channels. The second part tackles the problem of communication between the vehicles in a formation network using an hybrid solution that resorts to the use of acoustic and optical modems. Two communication architectures, synchronous and asynchronous, are proposed and solutions based on Finite State Machines are devised to supervise the interaction between vehicles, avoiding deadlocks. The performance obtained with the proposed solutions is accessed in simulation and the results are analysed and discussed.

Keywords: Cooperative Path Following, Network Motion Control, Marine Vehicle Control, Acoustic Communications, Optical Communications

1. Introduction

1.1. Motivation

Since the beginning of humanity there is a desire to explore the unknown. Throughout history this desire has had many sources from finding better life conditions or personal or collective enrichment to mere curiosity of the unknown and the willingness to learn more about what is around us. This is evident in the movements of the first humans when they left the African continent and in many conquests of emperors and kings and in the maritime explorations that led to the discovery of the maritime route to India, and the American continent by the Iberian nations.

After the exploration of most of the land on earth humans turned their eyes to what was under the sea and to the sky, for example the discovery of different deep-sea environments and creatures, and the invention of aircraft and spacecraft, respectively. The exploration of the skies ended up winning more attention likely due to the harsh conditions and technological challenges set forth by the deep-sea exploration. In particular, due in part to last century boost by the two world wars and by the cold war, aircraft and spacecraft technology has reach a high level of development that took humans to places never visited before.

Nowadays there are probes and telescopes that are being used to explore space and there are worldwide substantial human and financial resources invested in space industry. However, excluding the offshore oil industry, the investment in deep-sea exploration has been and continues to be much less than that in the space exploration, in spite of the fact that a large part of the deep-sea is still unknown to us.

Nonetheless, there are also many advantages in deep-sea exploration. One of the large challenge for the Humanity will be the future resource scarcity due to the nowadays extraction rate of most resources, in particular minerals. A medium term solution could be the underwater extraction of resources since most of them can be found in the sea bottom. This together with the sustainable exploration of fisheries requires accurate mapping of the ocean bottom and the study and identification of the habitat of the different species.

One of the projects carried out in this area is *MORPH* (figure 1). This project, described in [1], was aimed at developing groups of autonomous underwater vehicles which are required to operate in areas where the visibility is low, obstacles are not known in advance, and a single vehicle would have very limited capabilities. The techniques enabling cooperative behaviour of the MORPH ensemble paved the way for the development of advanced multi-vehicle systems capable of executing data acquisition and habitat mapping tasks in complex 3D environments (such as canyons and rugged cliff areas) in the presence of reduced visi-

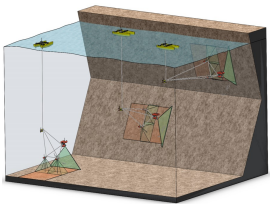

Figure 1: *MORPH* European project (source: Leture Notes A. Pascoal [17])

bility and natural unforeseen obstacles.

Another key project was *WiMUST*, presented in [2], which aimed at conceiving and designing an intelligent team of cooperative autonomous marine robots, acting as intelligent sensing and communicating nodes of a reconfigurable moving acoustic network, that could drastically improve the efficacy of the methodologies used to perform geophysical and geotechnical acoustic surveys at sea.

1.2. Functional Requirements and Objectives

To tackle the problems of ocean bottom mapping more efficiently it is far more efficient to use several vehicles simultaneously instead of one, because each vehicle can perform a specific task and only needs to carry the hardware necessary to accomplish that task as well as control and communications. This allows for the exploration of more remote places through the use of highly specialized vehicles that are smaller and lighter. For example in the *MORPH* project, each vehicle doesn't have to communicate directly with the command station installed on a surface vessel (figure 1) and the result of this decentralized mapping will be a more detailed image of the area in less surveying time.

In the above and similar projects there is a need to ensure that the vehicles will be able to move along desired paths in a coordinated manner while adopting a desired formation pattern. The later can change in time as a function of mission objectives and the type of terrain to be surveyed, in order to achieve optimal results in terms of data acquisition; other objectives include temporal constraints and energy efficiency, as well as the desire to avoid the loss of data due to communication errors caused, for example, by the vehicles too far away from each other or from a command station.

1.3. Technical Requirements

For cooperative motion control purposes, one possible approach is to resort to cooperative path following strategies. This entails two steps: i) design of a path following controller for each vehicle to drive it to it's assigned path at a desired speed, and ii) coordination of the vehicles along their paths by negotiating their speeds about the desired nominal values by exchanging data over a supporting communications network.

1.4. State of the Art

Recent technological developments have propelled autonomous marine vehicles to play an ever-increasing role in the underwater surveying and exploration creating a great interest in motion control for Autonomous Surface and Underwater Vehicles (AUV) [9], and [5], which is nowadays a very active research area. In particular, in the past decades, the scientific community has focused the attention on the topics of control of single and multiple ocean vehicles. In the literature, one can find many publications that tackle the problem of control of underactuated marine vehicles, see e.g., [21], [19], and [15]. Notice that by underactuated marine vehicle it is understood a vehicle that cannot directly actuate all degrees of freedom, e.g. typically a boat is able of generate forward force, along the x axis, surge direction, and torque about z axis, yaw angle, leaving the sway movement without direct actuation. In [13], a solution is proposed to tackle the problem of following a straight line and [4] introduces a controller based on waypoint tracking for an underactuated AUV.

To enforce a single vehicle to follow a given reference curve there are essentially two possible approaches: Trajectory-Tracking and Path-Following. The approach that will be taken in this work is the path-following approach [11, 3, 18]. These topics have been tackled by the control community in the last 3 decades and there is nowadays a solid number publications available on the topic. To refer just a few, the work in [10] proposes an attitude and position tracking controller and [6] presents trajectory tracking strategies for underactuated underwater vehicles.

Many publications have been dedicated to the topic of path-following, see for example [7], [14] and references therein. In [25], it is proposed a novel and improved strategy based on line-of-sight (LOS) for adaptive trajectory tracking control of an underactuated AUV subjected to highly coupled nonlinearities, uncertainties induced by ocean currents, and saturated inputs. Further results on line-of-sight and integral line-of-sight (ILOS) are provided in [8] where an extensive analysis of this guidance method for path-following tasks of underactuated marine vehicles, operating on and below the sea surface is presented. These technique will be further exploited in the present work, where we will develop a path-following controller in 2-D for the Medusa vehicle [11, 3, 18].

As mentioned before, two main techniques will be required to tackle the problem of cooperative control of multiple vehicles: Cooperative Motion Control and Networked Motion Control. To implement the first, a discrete time consensus algorithm will be used, on top of the vehicles' local path-

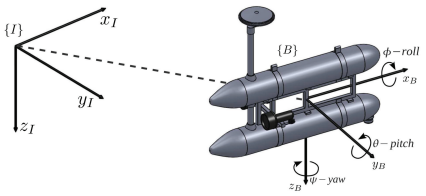

Figure 2: Reference frames and notation used (source: Ribeiro [23])

following controllers, to command and synchronize the overall vehicle formation.

For Networked Motion Control in ocean robotics there are three main ways of approaching the problem of the communication network: radio links while at surface and acoustic networks and optical networks underwater. The ones that are most used are radio links (used above water) and acoustic networks (used underwater), due to the long range coverage of these channels and to the range limitations of the optical networks. However there are advantages in the use of optical networks, based on green and blue lasers, and LEDs for undersea communications [24], such as allowing for a higher transmission rate and being more cost efficient [12]. The price to be payed it is the high directionality of lasers and therefore it will be required to point the emitter towards the reception devices, which could be designed to offer different reception aperture angles, as a function of the desired application. The problem of the impact of the directionality of the communication devices on the overall vehicles' formation will be dealt with in the present work. As far as we know, this is the first time that such a problem is tackled formally.

2. Vehicle Model Characterization

In this section we will characterize the dynamic model of the vehicles that will be used in this work.

2.1. Coordinate frames

We define an earth-fixed or inertial frame as $\{I\}$, placed somewhere in the mission scenario, and the body-fixed frame as $\{B\}$, attached to the vehicle, typically with its origin at the center of mass. The first is composed by the orthonormal axes $\{x_I, y_I, z_I\}$ and the second is composed by the orthogonal axes $\{x_B, y_B, z_B\}$ as represented in Figure 2.

In general, a marine vehicle can move in 6 degrees of freedom, thus 6 independent coordinates are needed to describe its position and orientation. The first three are the linear position coordinates (x, y, z) and other three are the Euler angles (ϕ, θ, ψ). Besides defining the position and the orientation we need to define the velocities, forces and torques applied to the vehicle body [16]. As such: The position of the origin of $\{B\}$ expressed in $\{I\}$ is represented by $\eta_1 = [x, y, z]^T$; The angles that parameterize locally the orientation of {B} with respect to {I} are $\eta_2 = [\phi, \theta, \psi]^T$, where ϕ is the roll, θ is the pitch and ψ is the yaw angle; The linear velocity of the origin of $\{B\}$ relative to $\{I\}$, expressed in $\{B\}$ is $\nu_1 = [u, v, w]^T$; The angular velocity of the origin of $\{B\}$ relative to $\{I\}$, expressed in $\{B\}$ is $\nu_2 = [p, q, r]^T$; The actuating forces on the vehicle expressed in $\{B\}$ are $\tau_1 = [X, Y, Z]^T$; The actuating moments on the vehicle expressed in $\{B\}$ are $\tau_2 = [K, M, N]^T$.

2.2. Kinematics

Now we are able to express the kinematics equations using the notation defined in section 2.1. This equations will result in

$$\dot{\eta} = J(\eta)\nu, \tag{1}$$

with

$$J(\eta) = \begin{bmatrix} {}^I_B R(\eta_2) & 0_{3\times3} \\ 0_{3\times3} & T(\eta_2) \end{bmatrix}, \tag{2}$$

where ${}^I_B R$ captures the relation between η_1 and ν_1 and corresponds to the rotation matrix that can be obtained by multiplying three single axis rotation matrices, each one representing a rotation over each of the axes of the body coordinate frame, with the convention zyx (yaw, pitch, roll), yielding

$${}^I_B R(\eta_2) = R_{z,\psi} R_{y,\theta} R_{x,\phi}. \tag{3}$$

The resulting rotation matrix is given by

$${}^I_B R(\eta_2) = \begin{bmatrix} c\psi c\theta & -s\psi c\phi + c\psi s\theta s\phi & s\psi s\theta + c\psi c\phi s\theta \\ s\psi c\theta & c\psi c\phi + s\psi s\theta s\phi & -c\psi s\theta + s\psi c\phi s\theta \\ -s\theta & c\theta s\phi & c\theta c\phi \end{bmatrix}, \tag{4}$$

where

$$\begin{aligned} c\cdot &= cos(\cdot), \\ s\cdot &= sin(\cdot). \end{aligned} \tag{5}$$

On the other hand T is the relation between η_2 and ν_2 and can be defined as

$$T(\eta_2) = \begin{bmatrix} 1 & s\phi t\theta & c\phi t\theta \\ 0 & c\phi & -s\phi \\ 0 & s\phi/c\theta & c\phi/c\theta \end{bmatrix}, \tag{6}$$

where

$$\begin{aligned} c\cdot &= cos(\cdot), \\ s\cdot &= sin(\cdot). \end{aligned} \tag{7}$$

This representation has a constraint because there is a singularity for $\theta = \pm 90°$. None the less, this is not a problem because the vehicle will operate about $\theta \approx 0$.

2.3. Dynamics

We now take into account the moments and forces that act on the marine vehicle and how they impact on the vehicle's motion. Since the dynamic equations become simpler if written in the body frame, Newton's law will be formulated in the $\{B\}$ frame. As such the rigid-body equation can be expressed as

$$M_{RB}\dot{\nu} + C_{RB}(\nu)\nu = \tau_{RB}, \tag{8}$$

where: the rigid body inertia matrix is M_{RB}; the Coriolis and the centripetal terms represented by C_{RB}; the external forces and moments are generalized in the vector τ_{RB}. The right-hander term can be expanded as $\tau_{RB} = \tau + \tau_A + \tau_D + \tau_R + \tau_{dist}$, where: τ is the vector of forces and torques due to thrusters or control surfaces, usually viewed as the control input; τ_A consists of the hydrodynamic forces and moments due to the added mass, given by $\tau_A = -M_a\dot{\nu} - C_A(\nu)\nu$; τ_D is the moments and forces generated by hydrodynamic effects due to lift, drag, skin friction, among others, yielding $\tau_D = -D(\nu)\nu$; τ_R is the sum of the restoring forces and torques due to gravity and buoyancy that are function of the bodys shape and the fluid density, that is, $\tau_R = -g(\eta)$; τ_{dist} is the term due to external disturbances induced by waves, wind, and ocean currents.

Replacing τ_{RB} on 8 by the respective components yields

$$\begin{aligned} M_{RB}\dot{\nu}+C_{RB}(\nu)\nu=\tau-M_A\dot{\nu}-C_A(\nu)\nu-D(\nu)\nu-g(\eta),\\ [M_{RB}+M_A]\dot{\nu}+[C_{RB}(\nu)+C_A(\nu)]\nu+D(\nu)\nu+g(\eta)=\tau+\tau_{dist},\\ M\dot{\nu}+C(\nu)\nu+D(\nu)\nu+g(\eta)=\tau+\tau_{dist}, \end{aligned} \tag{9}$$

where $M = M_{RB} + M_A$ is the inertia matrix including added mass and $C(\nu) = C_{RB}(\nu) + C_A(\nu)$ is the matrix of Coriolis an centripetal terms (including added mass).

2.4. Simplified Equations

We assume the vehicles considered in this work are only required to be controlled in the horizontal plane (*xy* plane). Thus, we can set $\theta = \phi = 0$ and the kinematics equations can be simplified to

$$\begin{aligned} \dot{x} &= ucos\psi - vsin\psi,\\ \dot{y} &= usin\psi + vcos\psi,\\ \dot{\psi} &= r. \end{aligned} \tag{10}$$

We can now split the forces generated by the thrusters in two: the external torque about the *z-axis* generated by the differential mode between the thrusters (τ_r) and the external force in $surge$ generated by the common mode between the thrusters (τ_u). As such, we have

$$\begin{aligned} \tau_u &= F_{ps} + F_{sb},\\ \tau_r &= (F_{ps} - F_{sb})l, \end{aligned} \tag{11}$$

where F_{ps} and F_{sb} are the forces produced by the portside and the starboard thursters respectively. The variable *l* represents the length of the arm with respect to the center of mass.

Disregarding the ocean currents, the vehicle only moves in the horizontal plane with the simplifications said before, the equations of dynamics can be simplified to

$$\begin{aligned} m_u\dot{u} - m_v vr + d_u u &= \tau_u,\\ m_v\dot{v} + m_u ur + d_v v &= 0,\\ m_r\dot{r} - m_{uv}uv + d_r r &= \tau_r, \end{aligned} \tag{12}$$

with

$$\begin{aligned} m_u &= m - X_{\dot{u}}, & d_u &= -X_u - X_{|u|u}|u|,\\ m_v &= m - Y_{\dot{v}}, & d_v &= -Y_v - Y_{|v|v}|v|,\\ m_r &= I_z - N_{\dot{r}}, & d_r &= -N_r - N_{|r|r}|r|,\\ m_{uv} &= m_u - m_v. \end{aligned} \tag{13}$$

The m_u, m_v, m_r and m_{uv} are mass and hydrodynamic added mass, respectively, and d_u, d_v, d_r are the hydrodynamic damping effects.

2.5. Vehicle Characterization - The Medusa

The vehicles considered in this work are the the *MEDUSA*-class autonomous vehicles. These are semi-submerged or submerged vehicles developed at Institute for Systems and Robotics of the Laboratory of Robotics and Systems in Engineering and Science (ISR/LARSyS) of the Instituto Superior Técnico of the University of Lisbon, Portugal. These vehicles are able to complement each other because they can carry different types of hardware, complementary among them, allowing for them to execute a very wide range of missions.

The parameters necessary for this model were initially obtained by dos Santos Ribeiro [22] and were later tuned in sea trials.

3. Cooperative Path Following

3.1. Single Vehicle Control

3.1.1 Yaw Controller - LQR

To develop and tune the *yaw* controller we choose the Linear Quadratic Regulator (*LQR*) control design technique. The objective of the *LQR* is to minimize the value of the cost functional

$$J = \int_{t=0}^{\infty} (x^T Q x + u^T R u) dt. \tag{14}$$

Deciding a set of reasonable weights for the problem at hand that is, selecting Q and R, is the key issue with this approach. As such, it

was assumed $Q = C_q^T C_q$, and as a starting point it was assumed that the entries of Q and R are the inverse of the reasonable allowed maximum, defined by the designer based on physical insight, of the variables being considered.In this case, $C_q = [|1/v_{max}|, |1/r_{max}|, |1/\psi_{max}|]$ and $R = |1/\tau_{max}|$.The steady state solution of the *LQR* problem can be determined by finding the unique positive definite matrix P that satisfies the algebraic *Riccati* equation,

$$A^T P + PA - PBR^{-1}B^T P + Q = 0. \quad (15)$$

At the end of this process it will be derived a gain matrix *K*.

The proposed control solution eliminates the sway speed, v, feedback (by setting $k_v = 0$) because this variable is difficult to measure, requires expensive equipment and, therefore, is not always available to be used in the controller.

It was concluded that the impact of the *sway* feedback is quite small given that both the set of eigenvalues and the time responses are quite similar (converge in less than 4 seconds and without oscillations) with or without the feedback of this variable.

3.1.2 Speed Controller

For path following purposes it is required to control the surge speed of the vehicle according to a desired speed.

We now design a speed controller to make the actual surge speed to track a desired reference speed that depends on the nominal speed adopted and the corrections introduced by the cooperative control law, as will be explained later.

In what follows the problem of forward speed control is tackled in a nonlinear setting. Consider the simplified dynamic model $F_p - \beta u|u| = m\dot{u}$, where F_p is the force generated by the thrusters and β is the damping coefficient of the vehicle along the surge direction.

Let *u* and u_d denote the true speed and the desired speed of the vehicle, respectively. Further let $e = u - u_d$ denote the speed tracking error. Simple computations yield the following equations

$$\begin{aligned} \dot{e} &= \dot{u} - \dot{u}_d, \\ \dot{e} &= \frac{F_p}{m} - \frac{\beta}{m} u|u| - \dot{u}_d. \end{aligned} \quad (16)$$

We adopted the control law $F_p = \beta u|u| - m\dot{u}_d - mke$, where *k* is a positive constant, from which we obtain $\dot{e} = -ke$.

Since the derivative of *e* is *e* multiplied by negative constant $(-k)$ the error (*e*) always goes to zero, in other words, *u* goes to u_d.

3.1.3 Path Following

Path Following consists of the task of following a specific spatial reference with a speed defined a priori, in other words, following a path with a certain speed. In this workthe tracking will be performed in the x-y plane and a yaw angle command will be used to control the vehicle's direction. For this reason, at each instant, a reference value of the yaw angle will be computed and supplied to the yaw controllerThe next sections aim to determine the yaw command using a guidance law called line-of-sight, for planar movements, and to show the feasibility of using this technique in calculating this reference.

The use of a guidance law based on line-of-sight with integral action will also be analyzed. This guidance law makes adjustments in order to correct the tracking errors by introducing integral action in the calculation of the control.

3.1.4 Line-of-Sight

The guidance law named line-of-sight (*LOS*) starts by considering the vehicle reference point (*rp*), usually the center of mass or any other point of interest on the vehicle, and uses it to calculate the point (*p*), closest to the vehicle reference point, on the curve to be followed. Assuming 0 vehicle sway velocity, for the tracking to be as close as possible to the reference path, first, draw the tangent to the path at point *p*. Then, finds the point *Dp* at a distance Δ on the tangent to the path. This will be point to which the vehicle will have to point in order to follow the reference path according to the line-of-sight guidance law. Thus, it is possible to calculate the reference yaw from the equation

$$yaw_{ref} = tan^{-1} \frac{y_{DP} - y_{rp}}{x_{Dp} - x_{rp}} \quad (17)$$

Which is equivalent to

$$yaw_{ref} = tan^{-1} \frac{d}{\Delta} + \alpha_{line} \quad (18)$$

where α_{line} is the angle that the tangent to the line to be followed makes with the xx axis. This last expression inspired by [8] will be useful for introducing the integral effect. This geometry can be inferred from the following figure

Simulating this law, it is possible to observe that different values of Δwill cause movements to approach the curve and follow it with very different characteristics from each other.

For smaller values of Δ, the effect on the guidance command caused by the guidance law will be more aggressive when compared to those obtained for higher values of the parameter Δ.

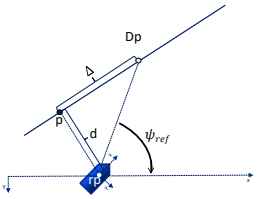

Figure 3: Line-of-sight guidance geometry.

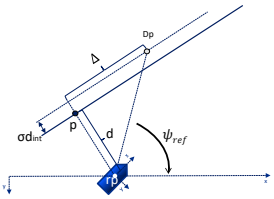

Figure 6: Integral line-of-sight guidance geometry.

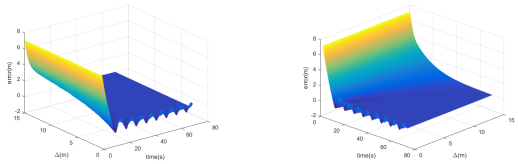

Figure 4: Tracking performance of the *LOS* guidance law, along straight lines for different values of Δ

Figure 5 presents the tracking performance of the line-of-sight guidance law, along an arc of a circumference.The use of line-of-sight with integral effect will be considered so that the accumulation of this error will eventually reduce, improving the overall performance of the guidance law.

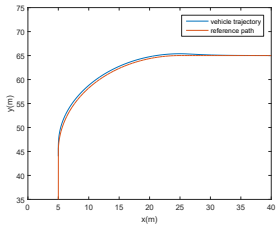

Figure 5: Tracking performance of the LOS guidance law, along a trajectory with a circular section.

3.2. Integral Line-of-Sight

Figure 6 shows the geometry as well as the new variables needed to calculate the Integral Line-Of-Sight (*ILOS*) guidance law, which will be explained next. Once more it is assumed in the computations that the vehicle sway velocity is 0.

In this geometry there is once again the concept of visibility distance Δ that is now applied to a straight line parallel to the tangent to the path. This line is then determined from the tangent to the path at point *p* which is shifted perpendicularly by an offset (d_{int}) multiplied by a parameter σ (a gain that weighs the integral of the error). This new component of the guidance law will compensate for the vehicle's tracking error and will facilitate its correction. The yaw angle is thus determined using

$$yaw_{ref} = tan^{-1}\frac{d\sigma * d_{int}}{\Delta} + \alpha_{line} \qquad (19)$$

and the integral effect will be computed through the following differential equation

$$\dot{d}_{int} = \frac{\Delta * d}{(d + \sigma * d_{int})^2 + delta^2}. \qquad (20)$$

The introduction of the integral effect in the guidance law *LOS* requires a detailed analysis of the impact of the parameter σ on the vehicle error in with respect to paths composed of straight lines and curves. The results obtained in the simulations carried out to analyze the convergence to straight lines, function of the parameter σ, and assuming $\Delta = 5.0$ m are shown in Figure 8. These simulation results were obtained with the nonlinear model of the vehicle.

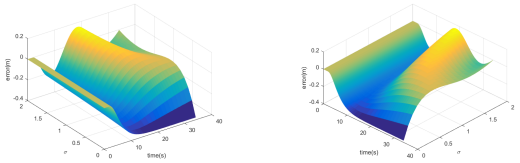

Figure 7: Switch from a straight line to a curve, function of the parameter σ for $\Delta = 5.0$ m.

Applying this guidance law, the result depicted in Figure 8 was obtained for circular paths and with the nonlinear model of the vehicle.

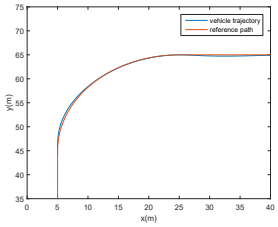

Figure 8: Tracking performance of the ILOS guidance law, along a trajectory with a circular section.

As seen, the *ILOS* computation allowed the vehicle to better follow a non-straight line path. Despite these positive results, it is also necessary to emphasize that in the transition between the circular section and the straight line, this guidance law displays and oscillatory behaviour and is unable to converge to the path as quickly as the *LOS*.

4. Cooperative Path Following

For missions involving more than one vehicle, for example to obtain acoustic images of the ocean bottom by a formation of underwater vehicles, it will be required to coordinate their motion along desired paths. To this end each vehicle will have access to a description of its path and, indirectly,

to descriptions of the paths of neighbouring vehicles. In Cooperative Path Following coordination is achieved by actuating on each vehicle forward's velocity, i.e. surge speed. Although there are different approaches in the literature to tackle this problem, most them are based on the same coordination equation whereby the reference velocity for i^{th} vehicle, u_i, is given by

$$u_i = u - K_u K_{sn}(S_i - \sum_{j \neq i} S_j) \qquad i = 1, 2, ..., N. \tag{21}$$

In the above, N is the number of neighbour vehicles communicating with vehicle i, K_u is a gain that translates distance between vehicles along the respective paths into velocity, u_f is the desired common formation speed, and K_{sn} is a gain that compensates for the scaling introduced by the curve parameterization. The S_j's are the curve parameters for the different neighbours that describe the successive locations of the different vehicles along the paths.

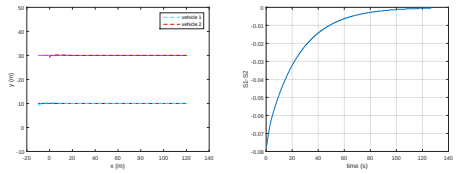

Figure 9: Simulation for two vehicles

This was the parameterization used in the simulations presented next for 2 vehicles. In what follows each vehicle will locally run a *ILOS* guidance law for path following purposes being the forward velocity controlled by the coordination algorithm.

5. Network Motion Control

5.1. Vehicles' Location Estimators

In order to keep the desired formation shape along the reference path is fundamental for each vehicle to know the location of its neighbour vehicles' in the formation in such way that the communication graph of the formation is at least connected, see [20]. However, in order to reduce the exchange of data between vehicles to a minimum level, each vehicle will have to use local estimators of the location on the path of its neighbour vehicles', i.e. the current value of the path parameter, of its neighbors and of itself in order to regulate the forward speed to keep the desired formation pattern. The solution adopted in this work it is based on the one developed in [20].

5.1.1 Simulations of the Estimators

For these simulations 3 vehicles were considered totally connected to each other (see communication graph of Figure 10). One of the values tested

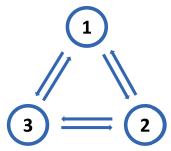

Figure 10: Network where all nodes are connected to each other

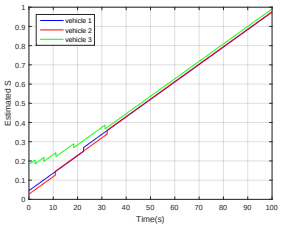

Figure 11: S_{est} for the simulation with $th = 0.02$

for the threshold was $th = 0.02$. in the parametrization used this value is equivalent to a maximum discrepancy of $2.2m$ (in absolute value) between the estimated and the actual vehicle's position projected on the path. Note that the fact that information is exchanged only occasionally has an influence on the overall system performance. As can be seen, in some occasions there are sharp jumps in the values of S_{est}. This is caused by the activation of the switch that replaces the value that is in the integrator of the estimator with the value S_{real}, as a consequence of the communication between vehicles.

On the other hand, it is also possible to note that these jumps are approximately of the same size. This is due to the existence of a common threshold and because communications are instantaneous, which implies that the jump will have, in absolute value, size equal to *th*.

Thus, as S_{est} is influenced by *th*, it will allow an error of $+/-0.02$ in relation to the actual location of the neighbour vehicles which will cause the vehicle to converge to a weighted average of the locations where it estimates that the neighbour vehicles are.

All of this will lead to the final formation shape not being exactly the desired one because each vehicle will converge to a location given by the average of the estimates of the other vehicles locations obtained from local estimators and not the average of the actual vehicles' locations.

Furthermore, it should be kept in mind that for vehicles the convergence was achieved because, after a certain time, the values of u_{ref} are approximately equal to the desired formation speed, however this convergence does not guarantee that the formation converges to the pre-defined configuration due to the reasons previously discussed.

Simulations for extreme cases and it's analyses can be found in the thesis.

5.2. Communications

In order to enable communication between two vehicles it is required that the optical modems of both are pointing towards each other. Thus, at each vehicle, the estimate of the position of the neighbourinhg vehicle obtained using the estimator described before can be used to compute approximately the orientation of the line joining the two vehicles. Let θ be the angle that a modem makes with the *x* axis of the corresponding vehicles body frame. In order to establish communication with the neighbour vehicle the current vehicle's modem angle can be obtained from $\theta = tan^{-1}\frac{x_2 - x_1}{y_2 - y_1} - yaw_1$, where x_c and y_c are the current vehicle actual position coordinates, ψ_c is the current vehicle *yaw* angle and x_n and y_n are the estimated values of position of the neighbour vehicle with which the current vehicle is trying to communicate to.

This approximation of the modem angle, may not be sufficient to find the neighbour vehicle modem antenna as the emitter only has a 20 degree aperture angle. Thus, it will be required for the modems to rotate and perform a local search.

For this search it was considered good solution to rotate the modems with time in both directions in an arc of 180 degrees centered at the approximate angle θ. This solution it's based on the assumption that the vehicle has some information about the others and the others are not too far away from their path.

5.2.1 Finite State Machines

We propose the use of finite state machines to model and supervise the communications between the vehicles in the formation. We will use one *FSM* per vehicle.

We propose two possible strategies to enable communication between the vehicles. The first one will be called the Synchronous Communications Strategy (*SCS*), similar to the one presented in the paper [20]. In this communication strategy, each vehicle will have a number of estimators (N_e) such that $N_e = N_c + 1$. Where N_c is the number of bidirectional connections that each vehicle has and the extra estimator is the estimator that each vehicle has for itself.

The second will be called Asynchronous Communication Strategy (*ACS*) because, instead of each vehicle having only one estimator of its own, it will have N_c estimators of itself, each one synchronized with the estimator of itself resident in each of the vehicles to which it is directly connected in the network. So, in this case, the number of estimators it is larger and will be $N_e = 2 \times N_c$.

An in depth analysis of the two strategies can be found in the master thesis, along with working examples of the respective architecture.

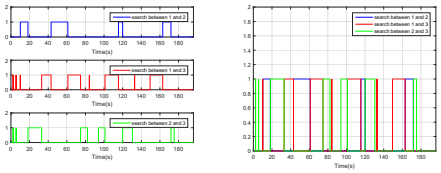

Figure 12: Activation signal between pairs of vehicles.

In complex networks when discrete event systems such as finite state machines are operating in parallel with communication between them, they no longer can be seen as isolated and the overall set is equivalent to a finite state machine that results from the concatenation of all of them through the connections provided by the communications. Thus, the possibility of deadlocks may emerge, that is, there are situations in which the machines can get stuck waiting for each other in the current states from which there will be no progress.

For the case of 3 vehicles, the state machines that were presented in the thesis were designed so that their joint operation does not give rise to *deadlocks*.

However when the problem is scaled and more vehicles are included in the network, it becomes much more complex to ensure that the finite state machines do not block.

Thus, in each finite state machine an extra state has been added to each *Wait* state to which the *FSM* will transit if it has been in *Wait* state for more than a certain time (*timeout*). This extra state is used to send a signal cancelling the communication request and make sure the other vehicle hasn't sent a communication request during the state transition.

6. Simulations for Asynchronous Communication Strategy

For the paths chosen, assuming $th = 0.01$, the maximum mismatch angle will be $\alpha_{desf} = tan^{-1}\frac{2.028}{5} = 22,07°$.

This angle is larger than that which allows the communication between modems (maximum deviation of +/- $10°$) thus, for the desired formation, this th is larger than the one that should be used because, if possible, it should be ensured that maximum estimation errors under normal operating conditions would not generate time consuming searches among modems. Despite the above, this was the threshold value used so that it was not necessary to induce external disturbances in the simulation to test the behaviour of the search between modems.

As is possible to observe in Figure 12, there is no overlap between periods of search for different connections. This demonstrates the smooth oper-

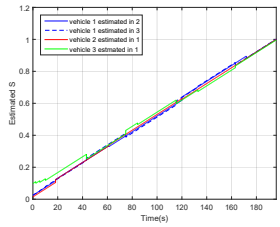

Figure 13: Evolution of S_{est} in the simulation seen from the perspective of vehicle 1.

ation of finite state machines and their capability to resolving conflicts.

Figure 13 presents the graphs of S_{est} curve parameter for vehicle 1 in this simulation.

In this case, evident difference is that the jumps are no longer of duration equal to that of the threshold th, which is caused by the delay between a vehicle realizing that it needs to communicate and the communication actually taking place and due to the bidirectional characteristics of the communication.

As might be expected, the different sized jumps that can be seen in the S_{est} graphs are also mirrored in the graph of u_{ref}.

More details of how the simulation was built and a more in depth analyses of the results can be found in the master thesis.

7. Conclusions

This work aimed to study the use of mixed acoustic and optical communications as a method of data transmission in a formation of ocean vehicles controlled resorting to the Cooperative Path Following control technique.

To address this problem, we started by defining the required coordinate frames and expressing the kinematic and dynamic equations that describe the motion of a vehicle in a fluid, simplifying these equations later.

Then the problem of designing a motion controller for the Medusa vehicle in the horizontal plane was addressed. This was developed based on two controllers, one for the *yaw* angle and another one for the forward speed, *surge*.

Next the Path Following problem was addressed, where the Line-of-Sight and Integral Line-of-Sight strategies were studied. The first caused the vehicle to display a constant error when tracking a curve. To solve this problem, the second strategy was applied and was required a slight compromise in the quality of the convergence of the vehicle to a straight line. To address the problem of Coordinated Motion Control, in this case Coordinated Path-Following we resort to a consensus approach acting on the vehicle's forward reference speed, the surge motion.

The next step was to develop the vehicle location estimators based on the solution developed in [20] and study several values of the estimators' threshold th from which it was possible to conclude that this parameter is the factor that most influences the performance of the simulation when it reaches an equilibrium.

Then it was designed, for each vehicle, an independent Finite State Machine (*FSM*), and two architectures were proposed, the Synchronous Communication Strategy (*SCS*) and the Asynchronous Communication Strategy (*ACS*).

Finally, simulations of the proposed strategies were carried out to access the vehicles' formation response and their impact in the overall formation performance.

It was then concluded that the use of ACS is preferable because it uses communication and search time in a more efficient way and allows the correction of estimation errors less than th ,in case a vehicle receives communication requests from its neighboring vehicles, in addition to that, communications are more independent of each other, which can be advantageous for larger networks. However, both solutions are feasible with a suitable choice of the estimators' thresholds th's.

References

[1] The MORPH Project: Marine Robotic System of Self-Organising, Logically Li, nked Physical Nodes, January 2019.

[2] The WIMUST Project: Widely Scalable Mobile Underwater Sonar Tecnology (WiMUST), January 2019.

[3] A. P. Aguiar and A. Pascoal. Cooperative control of multiple autonomous marine vehicles: Theoretical foundations and practical issues. In G. Roberts and R. Sutton, editors, *Further Advances in Unmanned Marine Vehicles*, chapter 6, pages 255–282. The Institution of Engineering and Technology, IET, 2012.

[4] A. P. Aguiar and A. M. Pascoal. Dynamic positioning and way-point tracking of underactuated auvs in the presence of ocean currents. In *Proceedings of the 41st IEEE Conference on Decision and Control, 2002.*, volume 2, pages 2105–2110 vol.2, 2002.

[5] J. Albiez, S. Joyeux, C. Gaudig, J. Hilljegerdes, S. Kroffke, C. Schoo, S. Arnold, G. Mimoso, P. Alcantara, R. Saback, J. Britto, D. Cesar, G. Neves, T. Watanabe, P. Merz Paranhos, M. Reis, and F. Kirchner. Flatfish - a compact subsea-resident inspection auv. In *OCEANS 2015 - MTS/IEEE Washington*, pages 1–8, 2015.

[6] F. Alonge, F. D'Ippolito, and F. M. Raimondi. Trajectory tracking of underactuated underwa-

ter vehicles. In *Proceedings of the 40th IEEE Conference on Decision and Control (Cat. No.01CH37228)*, volume 5, pages 4421–4426 vol.5, 2001.

[7] M. Breivik and T. I. Fossen. Guidance-based path following for autonomous underwater vehicles. In *Proceedings of OCEANS 2005 MTS/IEEE*, pages 2807–2814 Vol. 3, 2005.

[8] W. Caharija, K. Y. Pettersen, M. Bibuli, P. Calado, E. Zereik, J. Braga, J. T. Gravdahl, A. J. Sorensen, M. Milovanovic, G. Bruzzone, and et al. Integral line-of-sight guidance and control of underactuated marine vehicles: Theory, simulations, and experiments. *IEEE Transactions on Control Systems Technology*, 24(5):1623–1642, 2016.

[9] K. Do and J. Pan. *Control of Ships and Underwater Vehicles: Design for Underactuated and Nonlinear Marine Systems*. Advances in Industrial Control. Springer London, 2009.

[10] O. Fjellstad and T. I. Fossen. Position and attitude tracking of auv's: a quaternion feedback approach. *IEEE Journal of Oceanic Engineering*, 19(4):512–518, 1994.

[11] R. Ghabcheloo, A. P. Aguiar, A. Pascoal, C. Silvestre, I. Kaminer, and J. Hespanha. Coordinated path-following in the presence of communication losses and time delays. *SIAM journal on control and optimization*, 48(1):234–265, 2009.

[12] P. Góis, N. Sreekantaswamy, N. Basavaraju, M. Rufino, L. Sebastião, J. Botelho, J. Gomes, and A. Pascoal. Development and validation of blue ray, an optical modem for the medusa class auvs. In *Underwater Communications and Networking Conference (UComms), 2016 IEEE Third*, pages 1–5. IEEE, 2016.

[13] G. Indiveri, G. Casalino, and M. Aicardi. Nonlinear time-invariant feedback control of an underactuated marine vehicle along a straight course. *Proceedings of the 2000 Conference on Maneuvering and Control of Marine Craft*, 33, 08 2000.

[14] L. Lapierre, D. Soetanto, and A. Pascoal. Nonlinear path following with applications to the control of autonomous underwater vehicles. In *42nd IEEE International Conference on Decision and Control (IEEE Cat. No.03CH37475)*, volume 2, pages 1256–1261 Vol.2, 2003.

[15] F. Mazenc, K. Pettersen, and H. Nijmeijer. Global uniform asymptotic stabilization of an underactuated surface vessel. *IEEE Transactions on Automatic Control*, 47(10):1759–1762, 2002.

[16] A. Pascoal. Lecture notes, autonomous vehicles: An introduction to modeling. *IST*, 2018.

[17] A. Pascoal. Lecture notes, cooperative motion control. *IST*, 2018.

[18] A. Pascoal. Lecture notes, medusa class systems implementation. *IST*, 2018.

[19] K. Pettersen and H. Nijmeijer. Global practical stabilization and tracking for an underactuated ship - a combined averaging and backstepping approach. *Modeling, Identification and Control*, 20, 10 1999.

[20] F. C. Rego, N. T. Hung, C. N. Jones, P. A. M., and A. A. Pedro. Cooperative path-following control with logic-based communications: theory and practice. *Navigation and Control of Autonomous Marine Vehicles*, page 187–224, 2019.

[21] M. Reyhanoglu. Control and stabilization of an underactuated surface vessel. In *Proceedings of 35th IEEE Conference on Decision and Control*, volume 3, pages 2371–2376 vol.3, 1996.

[22] J. Ribeiro. Motion control of single and multiple autonomous marine vehicles. Master's thesis, Instituto Superior Técnico, 2011.

[23] M. Ribeiro. Computer-based cooperative motion planning, programming, and control of autonomous robotic. Master's thesis, Instituto Superior Técnico, 2013.

[24] G. Spagnolo, L. Cozzella, and F. Leccese. Underwater optical wireless communications: Overview. *Sensors*, 20:2261, 04 2020.

[25] Y. Xia, K. Xu, Y. Li, G. Xu, and X. Xiang. Improved line-of-sight trajectory tracking control of under-actuated auv subjects to ocean currents and input saturation. *Ocean Engineering*, 174:14 – 30, 2019.